Chemical Physics Letters 578 (2013) 21–27

Contents lists available at SciVerse ScienceDirect

Chemical Physics Letters

journal homepage: www.elsevier.com/locate/cplett

The effect of the Coriolis coupling on H+ND reaction: A time dependent wave packet study

Sinan Akpinar *, Seda Surucu Hekim

Department of Physics, Faculty of Science, Firat University, 23169 Elazig, Turkey

ARTICLE INFO

Article history:
Received 11 January 2013
In final form 7 May 2013
Available online 27 May 2013

ABSTRACT

We present a quantum scattering calculation of initial-state-resolved reaction probabilities, integral cross section, initial state selected reaction rate constants and thermal rate constant for exchange and depletion channels of the H+ND reaction. The calculations are carried out using Coriolis coupling (CC) method on the modified NH_2 $\tilde{A}^2A_1$ potential energy surface(PES). The initial state selected reaction probabilities are calculated for 0.0–0.5 eV of collision energy range. The reaction probabilities for depletion channel shows some sharp and large resonances associated with long-lived collision complexes, as compared to exchange channel. Integral cross sections for both reactions depend strongly on initial rotational states. The calculated thermal reaction rate constant for the depletion channel is in a good agreement with the values previously obtained by the centrifugal sudden approximation, experimental and semiclassical results.

1. Introduction

It is well known that neglection of Coriolis coupling (CC) in quantum dynamical simulations of bimolecular reactions decreases the computational cost to a large extent [1]. But at the same time, computational accuracy and efficiency is also reduced to some extent. Recently, exact calculations including the CC have been carried out for various reactions in several theoretical investigations [2–11].

NH+H reaction and its isotopic variants play an important role in many gas-phase environments, particularly, those in combustion, atmospheres and even cold interstellar media. The NH radical is a potential target to understand noncatalytic radical mechanisms of ammonia formation. Therefore, it has been the subject to many theoretical and experimental studies. Qu et al. [12] and Adam et al. [13] measured room-temperature rate constants from a quasistatic laser-flash photolysis and laser-induced fluorescence system at low pressures for $NH(X^3\Sigma^-) + D(^2S)$ and $NH(a^1\Delta) + H(^2S)$ reactions, and their deuterated variants. These authors also computed two potential energy surfaces and calculated semiclassical cross sections, and rate constants. The reactants correlate with the NH_2 $\tilde{X}^2B_1$ and $\tilde{A}^2A_1$ doublet electronic states, respectively. The most accurate global potential energy surfaces for these two electronic states were obtained at the multireference-configuration interaction level, plus Davidson correction, via the aug-cc-pvqz atomic basis. The calculated reaction rates on these surfaces showed a good agreement with experimental results [12,13]. Akpinar et al. [14] and Defazio et al. [15] presented the quantum mechanical wave packet (WP), experimental and quasiclassical trajectory based results for the reactions of electronically excited $NH(a^1\Delta, v = 0)$ and electronically and vibrationally excited $NH(a^1\Delta, v = 1)$, respectively. The state-to-state dynamics of NH+H reaction has been studied for exchange and abstraction channels using quantum mechanical and quasiclassical methods [16] on the ground electronic state on $NH_2(X^2A'')$, which features a deep potential well and barrierless reaction pathway [17]. Defazio et al. presented the quantum dynamics of Renner–Teller and isotopic effects in $NH(a^1\Delta) + D(^2S)$ reactions. Renner–Teller (RT) interactions between the involved electronic states were taken into account via a semiempirical RT matrix element, and a real wavepacket method with coupled channel formalism [18] was employed for the dynamics. Surucu et al. [19,20] have recently reported the reaction kinetics using centrifugal sudden approximation for depletion and exchange channels of H+ND and D+ND reactive scattering, respectively.

In this Letter, we investigate the effect of the Coriolis coupling in the quantum calculations for the $ND(a^1\Delta) + H(^2S) \rightarrow \left\{ \begin{array}{c} N(^2D) + HD(X^1\Sigma_g^+) \\ NH(a^1\Delta) + D(^2S) \end{array} \right\}$ depletion and exchange reactions, respectively. CC calculations have been carried out for the initial rotational states $j_0 = 2, 3, 4, 5$ to get the reaction probabilities, cross sections, rate constants and thermal rate constant for exchange and depletion channels for the values of the total angular momentum quantum number J up to 33. The results have been compared to available experimental and previously calculated theoretical results.

* Corresponding author.
E-mail address: sakpinar@firat.edu.tr (S. Akpinar).

0009-2614
http://dx.doi.org/10.1016/j.cplett.2013.05.010

2. Theory

The Hamiltonian operator for an atom–diatom system in a body-fixed (BF) reference frame may be written in terms of reactant Jacobi coordinates (R,r,γ) as (ħ = 1).

$$\hat{H} = -\frac{1\partial^2}{2\mu_R \partial R^2} - \frac{1\partial^2}{2\mu_r \partial r^2} + \frac{1}{2}\left(\frac{1}{\mu_R R^2} + \frac{1}{\mu_r r^2}\right)\hat{j}^2 + \frac{[\hat{J}^2 - 2\hat{J}_z\hat{j}_z]}{2\mu_R R^2} - \frac{[\hat{J}_+\hat{j}_- + \hat{J}_-\hat{j}_+]}{2\mu_R R^2} + V(R,r,\gamma) \quad (1)$$

Here R is the distance between H atom and the center of mass of ND, r is the ND bond length, and γ is the angle between R and r. μ_R is the reduced mass of the H-ND system, μ_r is the reduced of ND molecule. $\hat{j}$ is the rotational angular momentum operator of ND molecule and $\hat{J}$ is total angular momentum operator. $\hat{J}_z$ and $\hat{j}_z$ are the operators corresponding to the z components of $\hat{J}$ and $\hat{j}$, respectively. The corresponding raising (lowering) operators, $\hat{J}_+(\hat{J}_-)$ and $\hat{j}_+(\hat{j}_-)$, are the responsible for Coriolis coupling. $V(R,r,\gamma)$ is the interaction potential in Ref. [13].

The state resolved reaction probabilities can be extracted by calculating the flux at a fixed surface of the time-dependent part of the wave function as

Table 1
Parameters of the calculations.[a]

Sinc initial WP:	Translational energy center	0.15 eV	
	R center and width	9 and 4	
	Smoothing parameter	0.01	
R range and number of grid points		1–15	139
r range and number of grid points		1.5–13	139
Number of associated Legendre polynomials		80	
Potential and centrifugal cut-off		0.44	
R and r absorption start at		12 and 10	
R and r absorption strength		0.01	
Flux analysis at r		9	

[a] Values in a.u., unless otherwise specified.

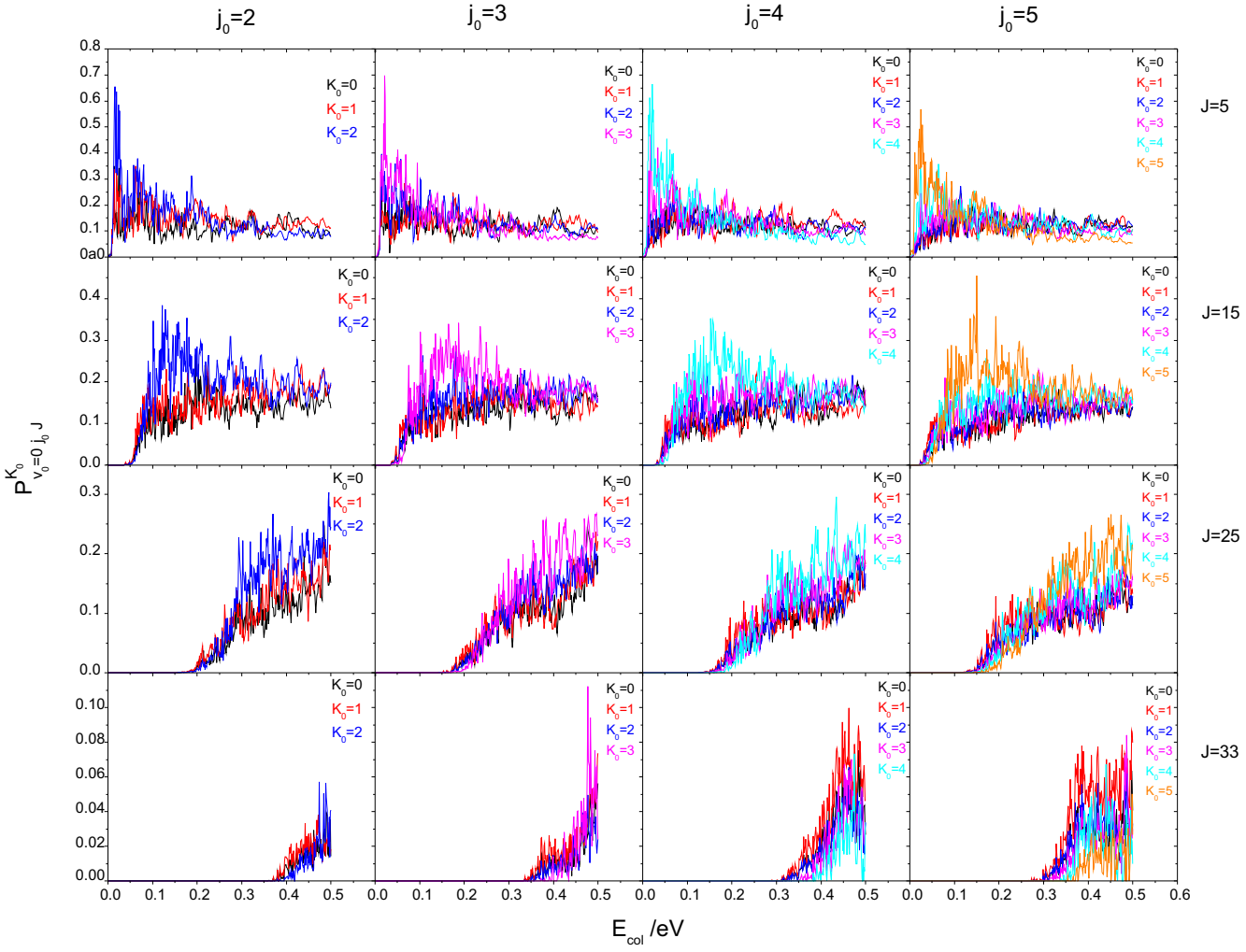

Figure 1. CC initial-state-resolved depletion reaction probabilities for different K_0 values calculated at $v_0 = 0$, $j_0 = 2, 3, 4, 5$ plotted for four different total angular momentum values as a function of collision energy.

$$P^{JK_0}_{v_0j_0}(E) = \frac{\hbar}{\mu_r}\mathrm{Im}\left\langle \Phi^{+}_{v_0J_0}(E)\middle|\delta(r-r_0)\frac{\partial}{\partial r}\middle|\Phi^{+}_{v_0J_0}(E)\right\rangle. \quad (2)$$

where $\Phi^{+}_{v_0j_0}(E)$ denotes the time-independent full scattering wave function. v_0 and j_0 are the initial vibrational and rotational quantum numbers of diatomic molecule. The J-dependent reaction probability is computed from the propagated wave packet as

$$P^{J}_{v_0j_0}(E_{col}) = \frac{1}{2j+1}[P^{JpK_0=0}_{v_0j_0}(E_{col}) + 2\sum_{K=1}^{\infty}P^{JpK_0}_{v_0j_0}(E_{col})] \quad (3)$$

where $p = \pm$ is the parity, $K_0 \leqslant \min(J, j_0)$ is the projection quantum number of both J and j_0 along z axis and E_{col} is the translational energy. It may be seen from Eq. (3) that the Coriolis term has effect on the second term in the equation. Therefore, in the present study, the initial rotational quantum number was started from 2. The total reaction probability for any selected initial quantum state v_0, j_0, K_0 is calculated by summing the state-to-state reaction probabilities over all final quantum states v, j, K. On the other hand, the reaction cross section for an initial state of v_0, j_0, K_0 is simply calculated by summing the total reaction probabilities over all available J states as

$$\sigma_{v_0j_0K_0}(E_{col}) = \frac{\pi}{2v_R E_{col}/\hbar^2}\sum_J(2J+1)\sum_{J=K_0}^{\infty}P^{J}_{v_0j_0}(E_{col}) \quad (4)$$

The initial state specific rate constant is obtained by Maxwell averaging the cross sections over all collision energy values as

$$k_{v_0j_0}(T) = \left(\frac{8}{\pi v_R k_B^3 T^3}\right)^{1/2}\int_0^{\infty} dE_{col}E_{col}e^{-E_{col}/k_BT}\sigma_{v_0j_0K_0}(E_{col}) \quad (5)$$

where k_B is the Boltzmann constant. Finally, the thermal rate constant is obtained by averaging the initial states rate constants by the Boltzmann probabilities $p_{vj}(T)$ of the initial states,

$$k(T) = \sum_{v_0j_0}k_{v_0j_0}(T)p_{v_0j_0}(T) \quad (6)$$

where

$$p_{v_0j_0}(T) = \frac{(2j_0+1)e^{-\varepsilon_{v_0j_0}/k_BT}}{\sum_{v_0J_0}(2j_0+1)e^{-\varepsilon_{v_0j_0}/k_BT}} \quad (7)$$

The term at the denominator of Eq. (7) denotes the reactant partition function of the internal states. $\varepsilon_{v0,j0}$ is the energy of the initial rovibrational state of ND.

3. Results and discussions

We used the quantum mechanical real WP and flux analysis method [21–22], to calculate the reaction probabilities, cross sections, rate constants and thermal rate constant for the H+ND reaction. A modified PES for $NH_2\tilde{A}^2A_1$ was employed in these

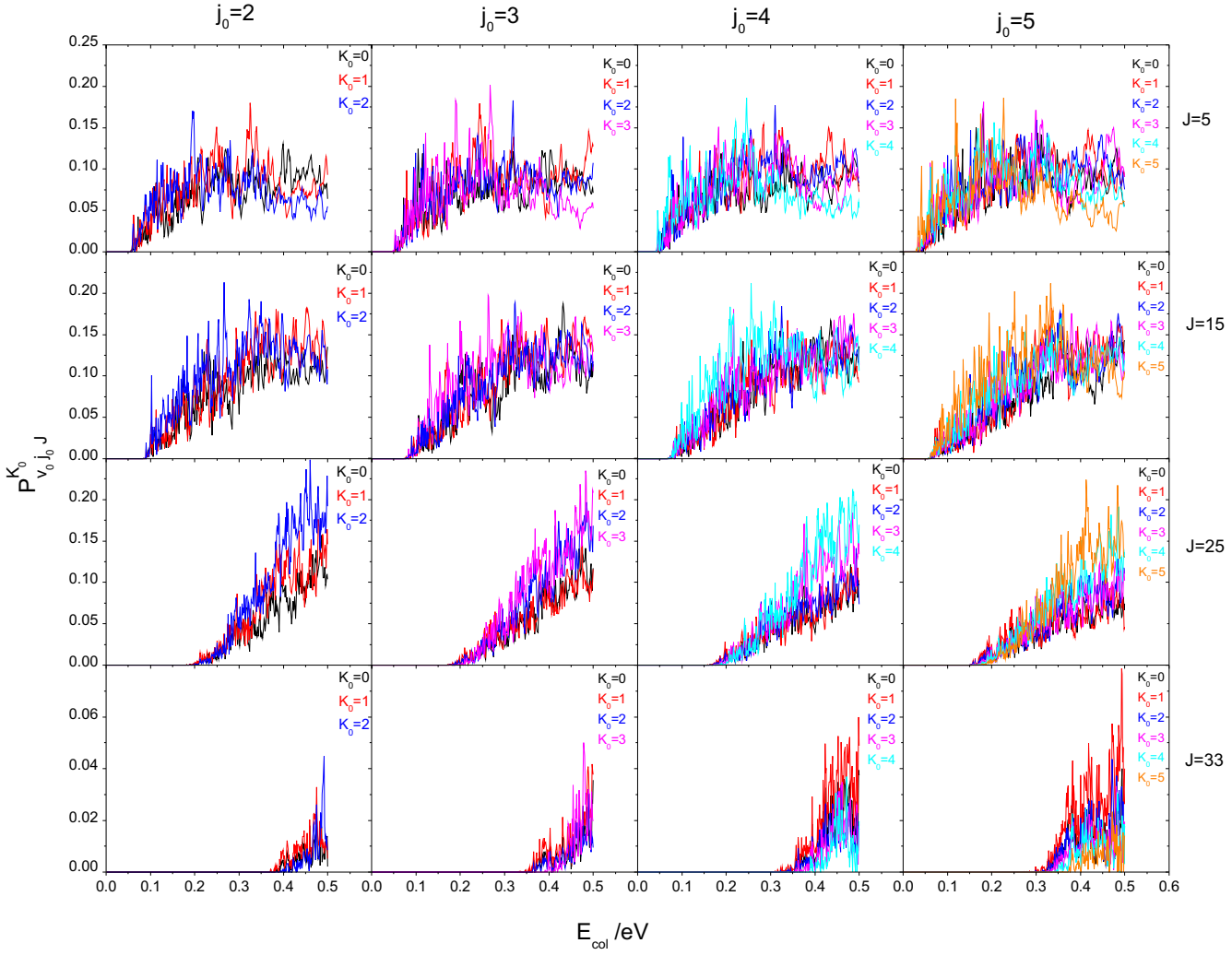

Figure 2. CC initial-state-resolved exchange reaction probabilities for different K_0 values calculated at $v_0 = 0$, $j_0 = 2, 3, 4, 5$ plotted for four different total angular momentum values as a function of collision energy.

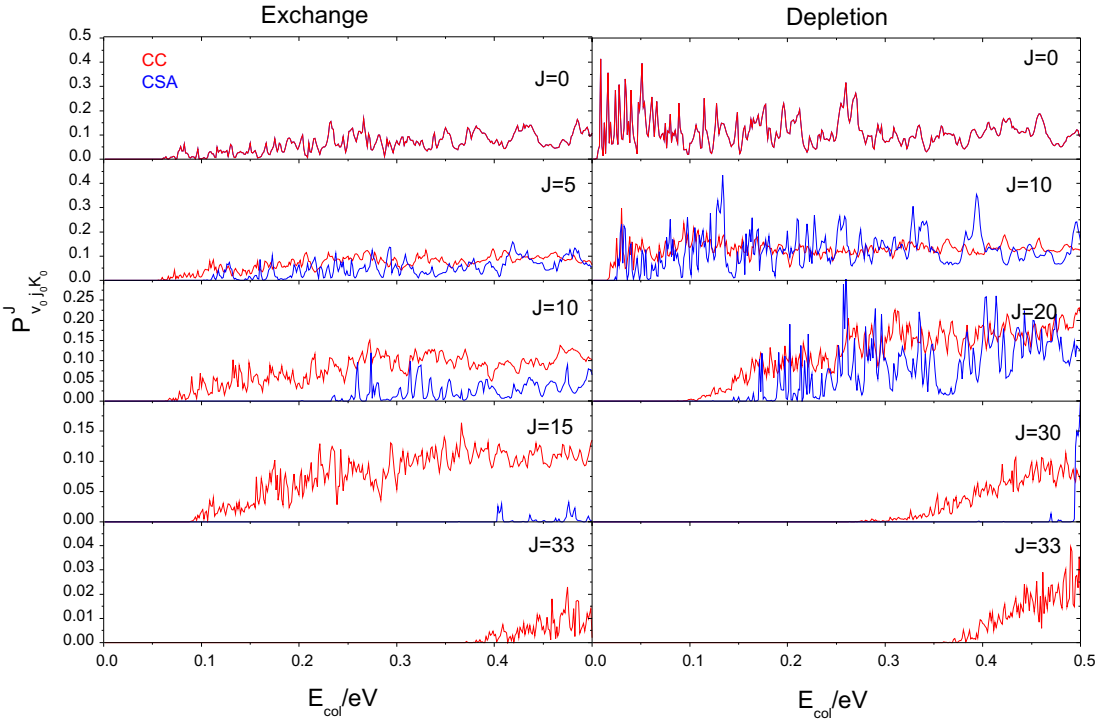

Figure 3. CC and CSA initial-state-resolved reaction probabilities as a function of collision energy at selected total angular momentum values for both depletion and exchange reactions.

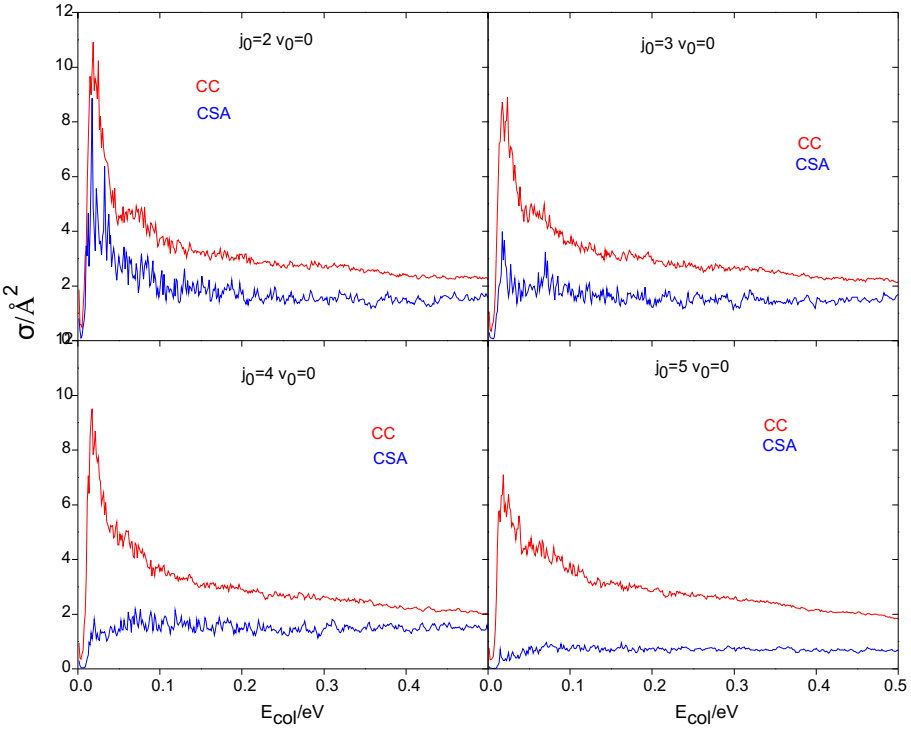

Figure 4. A comparison between CC and CSA cross sections of different initial rotational states for depletion reaction as a function of collision energy.

calculations [14]. The initial wave packet was set up in the *sinc* form [23] and a three-term Chebychev propagator [24] based on a shifted and scaled Hamiltonian operator has been used for the propagation of the wave function. We calculated CC initial-state-resolved reaction probabilities $P^{Jp}_{j_0K_0}(E_{col})$ for all K values, namely $J = K_0$, K_0+1, K_0+2, K_0+3,. . .,K. Note that the number of K is large

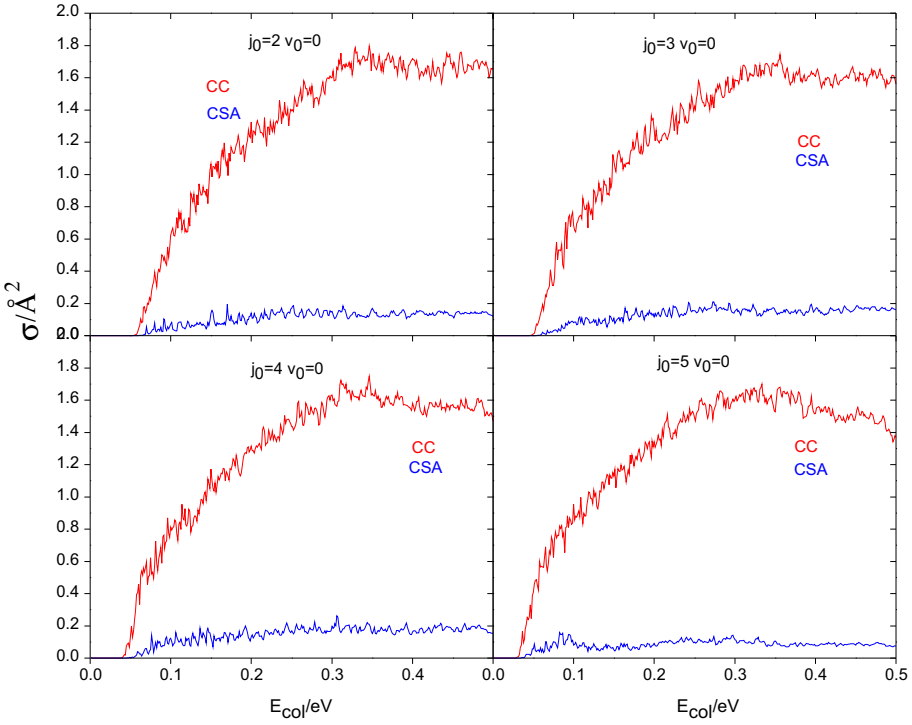

Figure 5. A comparison between CC and CSA cross sections of different initial rotational states for exchange reaction as a function of collision energy.

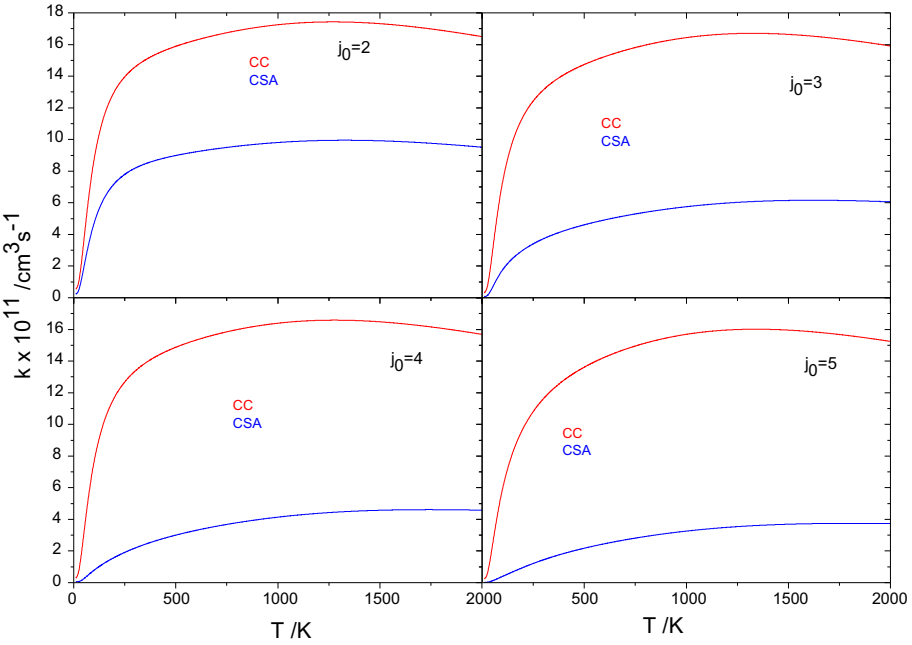

Figure 6. CC and CSA rate constants of initial rotational states for depletion reaction as a function of temperature.

in CC calculations, making computations rather expensive. The reactant diatom ND($a^1\Delta, v_0 = 0, j_0$) was considered to be in the first excited electronic state $a^1\Delta$, in the ground vibrational state $v_0 = 0$, and in the rotational state $j_0 \geqslant 2$ [14]. Many test calculations have been performed to check the convergence of the numerical parameters given in Table 1. The propagation of the wavepacket requires 80000 steps (iterations) to converge. CC calculations were performed using an MPI parallel code on 4XAMD Opteron 6174 processor where each process works on one K value.

The collision energy dependence of CC reaction probabilities calculated for different K_0 values are plotted in Figures 1 and 2 at $v_0 = 0$, j_0 = 2, 3, 4, 5 and J = 5, 15, 25, 33 for depletion and ex-

change channels, respectively. Although, the $\tilde{A}^2A'$ PES is barrierless for both channels, the exchange channel reaction probabilities show a threshold due to its endothermicity, but depletion reaction for $J = 0$ does not present any thresholds. All the probabilities for depletion channel show a strong and sharp oscillatory structure, attributed to long lived states, up to $E_{col} = 0.5$ eV and $J_{max} = 33$, due to the deep and wide potential wells. The reaction probabilities for depletion channel are generally higher than the exchange channel over the studied energy range. As seen in Figures 1 and 2 for both reactions, the oscillatory structure is reduced at high J values, as expected by the Coriolis-coupling averaging among many K states, and by the ND rotational excitation. This is due to the initial centrifugal terms $[J(J+1)+j_0(j_0+1)-2K_0^2]/2\mu_R R^2$. This term also effects the probability thresholds of both reactions.

Figure 3 shows a comparison of initial-state-resolved probabilities at selected total angular momentum $J = 0$, 10, 20, 30, 33 of depletion channel and $J = 0$, 5, 10, 15, 33 of exchange channel for initial quantum numbers $v_0 = 0$, j_0=2 and K_0=0 calculated by the Centrifugal Sudden Approximation (CSA) [19] and the present CC method. The values and the pronounced extent of the resonances peaks in the calculated probabilities for both reactions are very different for the CC and CSA calculations. The CC probabilities have richer, but less pronounced, resonance structures than the CSA ones, in particular in the low energy region. It can also be seen that the CC probabilities have slightly lower threshold energy than the CSA ones. As J increases for both reactions, the threshold shifts to higher energies and the resonance structure becomes less evident, particularly for CC calculations. It can be seen that reactive resonances are more pronounced for depletion channel as comperred to exchange channel. While CC probabilities at higher total angular momentum values are observed for exchange reaction, CSA probabilities are absent at the same total angular momentum values due to neglection of the Coriolis coupling effect.

A comparison of CC and CSA [19] cross sections of the H+ND ($v_0 = 0, j_0 = 2, 3, 4, 5$ reaction for the depletion and exchange reactions are presented in Figures 4 and 5 as a function of collision energy. To obtain the CC cross sections, the reaction probabilities were calculated for all the J values in the range $0 \leqslant J \leqslant J_{max}$. It can be seen from these figures that the behavior of the cross sections for both reactions is rather different. Because of nature of the $NH_2\tilde{A}^2A_1$ PES [13–14], the depletion cross section does not have a threshold for both CC and CSA results and cross sections decrease with increasing collision energy. But for the exchange reaction, reaction thresholds are seen for both the exact and approximate results. Also, the reaction cross sections increase with increase in collision energy as expected for an endothermic reaction, for this channel. The reaction thresholds decrease with increase in initial rotational quantum state of ND molecule. As shown in Figures 4 and 5, for both depletion and exchange cross sections, the CC cross section is larger than the CSA ones due to the Coriolis coupling effect. So, CC cross section has a greater effect in the exchange reaction than in the depletion channel. As the collision energy increases, the difference between the CC and CSA cross sections for exchange reaction become larger. Reason is that the effect of the Coriolis coupling terms (the K values) for exchange reaction is negligible for low collision energy. But it has a greater effect with increasing energy, which is in agreement with that of some other reaction systems [6,8,10,11]. It is important to note that for reactive systems, many K states are highly populated and have a significant contribution.

The calculated CC and CSA [19] initial state specified rate constants are shown in Figures 6 and 7 as a function of temperature for depletion and exchange reaction, respectively. The temperature dependence of the rate constants dramatically differ for both reactions. At lower temperatures, the differences between CC and CSA rate constants are relatively small, but as the temperature increases, large differences are observed. As can be seen, for depletion and exchange reactions, CC rate constants are larger than CSA rate constants for all initial rotational states in the studied range of temperatures. Both CC and CSA initial rate constants initially increase at lowest temperatures, then decrease slightly with increasing temperature reaching almost a constant value. Similar results were reported for the NH+H isotope variant of the reaction [14]. We also calculated the CC thermal rate constant including the 1/2 electronic degeneracy factor of both reactions using Eq. (7). For depletion channel, the CC thermal rate constant was compared with the experimental value [13], the semiempirical trajectory-surface hopping value [13] and the value obtained from CSA

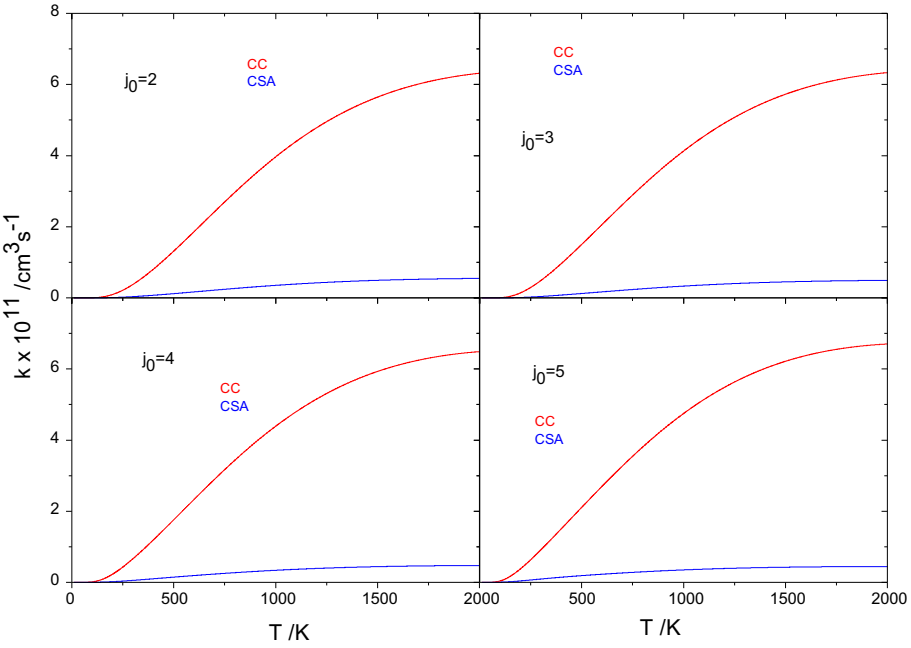

Figure 7. CC and CSA rate constants of initial rotational states for exchange reaction as a function of temperature.

calculations on the same PES [19]. In this Letter, the thermal rate constant at 300 K was calculated as 5.76×10^{-11} cm^3 s^{-1}. Our result is in good agreement with the experimental value of 8.14×10^{-11} cm^3 s^{-1}. In comparison, CSA and semiempirical trajectory-surface hopping calculations have reported values of 1.74×10^{-11} cm^3 s^{-1} and 7.74×10^{-11} cm^3 s^{-1}, respectively. The thermal rate constant for exchange channel has not been experimentally observed so far [13]. But the CSA thermal rate constant at 300 K was obtained as 0.35×10^{-12} by Surucu et al. [19]. Their value is at least 10 times lower than our values 3.33×10^{-12} obtained by CC method.

4. Conclusions

We have carried out detailed quantum mechanical Coriolis coupling calculations for the H+ND reaction on the modified $NH_2\tilde{A}^2A_1$ PES. It has been shown that it is possible to obtain CC initial-state-resolved reaction probabilities with respect to all K values. We found that the reactivity of the depletion reaction is far greater than that of the exchange reaction. The difference between CC and CSA cross sections becomes increasingly obvious with increase in the collision energy. The thermal rate constant result at 300 K agree quite well with the available experimental value. It is concluded that the CS approximation does not work for this system and higher values of K are required to obtain converged reaction cross sections.

Acknowledgements

Authors are indebted to Prof. Fahrettin GOKTAS, Dr. Aditya N. Panda and Dr. Enrico Bodo for many stimulating discussions on quantum wave packet theory. The numerical calculations reported in this Letter were performed on High Performance and Grid Computing Center (TR-Grid) machines at TUBITAK, ULAKBIM/TURKEY.

References

[1] W.L. Emlia, J. Comp. Chem. 31 (2010) 2827.
[2] A.J.H.M. Meijer, E.M. Goldfield, J. Chem. Phys. 110 (1999) 870.
[3] E.M. Goldfield, A.J.H.M. Meijer, J. Chem. Phys. 113 (2000) 11055.
[4] A.N. Panda, N. Sathyamurthy, J. Chem. Phys. 121 (2004) 9343.
[5] P. Defazio, C. Petrongolo, J. Chem. Phys. 127 (2007) 204311.
[6] T.S. Chu, K.L. Han, Phys. Chem. Chem. Phys. 10 (2008) 2431.
[7] P. Gamallo, P. Defazio, J. Chem. Phys. 131 (2009) 044320.
[8] S.J. Lv, P.Y. Zhang, K.L. Han, G.Z. He, J. Chem. Phys. 132 (2010) 014303.
[9] P. Gamallo, P. Defazio, M. Gonzalez, J. Phys. Chem. A 115 (2011) 11525.
[10] S.J. Lv, P.Y. Zhang, K.L. Han, G.Z. He, J. Chem. Phys. 136 (2012) 094308.
[11] N. Bulut, J. Klos, M.H. Alexander, J. Chem. Phys. 136 (2012) 104304.
[12] Z.-W. Qu, H. Zhu, R. Schinke, L. Adam, W. Hack, J. Chem. Phys. 122 (2005) 204313.
[13] L. Adam, W. Hack, G.C. McBane, H. Zhu, Z.-W. Qu, R. Schinke, J. Chem. Phys. 126 (2007) 034304.
[14] S. Akpinar, P. Defazio, P. Gamallo, C. Petrongolo, J. Chem. Phys. 129 (2008) 174307.
[15] P. Defazio et al., J. Phys. Chem. A 113 (2009) 14458.
[16] Z. Li, C. Xie, B. Jiang, D. Xie, L. Liu, Z. Sun, D.H. Zhang, H. Guo, J. Chem. Phys. 134 (2011) 134303.
[17] S. Zhou, D. Xie, S.Y. Lin, H. Guo, J. Chem. Phys. 128 (2008) 224316.
[18] P. Defazio, P. Gamallo, S. Akpinar, C. Petrongolo, Phys. Chem. Chem. Phys. 13 (2011) 8470.
[19] S. Surucu, G. Tasmanoglu, S. Akpinar, Mol. Phys. 110 (2012) 1525.
[20] S. Surucu, G. Tasmanoglu, S. Akpinar, Mol. Phys. (2012), http://dx.doi.org/10.1080/00268976.2012.664664.
[21] S.K. Gray, G.G. Balint-Kurti, J. Chem. Phys. 108 (1998) 950.
[22] A.J.H. Meijer, E.M. Goldfield, S.K. Gray, G.G. Balint-Kurti, Chem. Phys. Lett. 293 (1998) 270.
[23] M. Hankel, G.G. Balint-Kurti, S.K. Gray, Int. J. Quantum Chem. 92 (2003) 205.
[24] V.A. Mandelshtam, H.S. Taylor, J. Chem. Phys. 102 (1995) 7390.